Effects of Charcot-Marie-Tooth-linked mutations of the neurofilament light subunit on intermediate filament formation

Raul Perez-Olle, Conrad L. Leung and Ronald K. H. Liem*

Department of Pathology, Columbia University College of Physicians & Surgeons, 630 West 168th Street, New York, NY 10032, USA
*Author for correspondence (e-mail: rkl2@columbia.edu)

Accepted 4 September 2002
Journal of Cell Science 115, 4937-4946 © 2002 The Company of Biologists Ltd
doi:10.1242/jcs.00148

Summary

Neurofilaments (NFs) are the major intermediate filaments (IFs) of mature neurons. They play important roles in the structure and function of axons. Recently, two mutations in the neurofilament light (NFL) subunit have been identified in families affected by Charcot-Marie-Tooth (CMT) neuropathy type 2. We have characterized the effects of these NFL mutations on the formation of IF networks using a transient transfection system. Both mutations disrupted the self-assembly of human NFL. The Q333P mutant in the rod domain of NFL also disrupted the formation of rat and human NFL/NFM heteropolymers. The phenotypes produced by the P8R mutation in the head domain of NFL were less severe. The P8R mutant NFL co-polymerized with NFM to form bundled filaments and, less often, aggregates. Our results suggest that alterations in the formation of a normal IF network in neurons elicited by these NFL mutations may contribute to the development of Charcot-Marie-Tooth neuropathy.

Key words: Charcot-Marie-Tooth, Intermediate filament, Neurofilament, Assembly

Introduction

Charcot-Marie-Tooth (CMT) neuropathy is the most prevalent inherited sensory and motor neuropathy (approximately 1:2500 people in the general population). CMT has been classically subdivided in the demyelinating form (type 1 or CMT1) and the axonal form (type 2 or CMT2), mainly on the basis of the nerve conduction velocities. CMT does not affect the life span of the patients, but it may result in severe disability. CMT is a slowly progressive bilateral neuropathy with distal predominance. Symptoms due to loss of muscle control and muscle atrophy include weakness, foot drop, foot deformity, and leg deformity (Warner et al., 1999). CMT patients show a high degree of heterogeneity, both in the clinical presentation and at the genetic level. The existing clinical overlap between different types of CMT suggests the possibility of common pathogenic mechanisms. An interplay between demyelination and chronic axonal degeneration in the different types of CMT has been suggested. Mutations in different genes important for myelin formation and maintenance have been identified in CMT1 patients. These include mutations in peripheral myelin protein, PMP 22 (Roa et al., 1993), myelin protein zero, P0 (Hayasaka et al., 1993), connexin 32 (Bergoffen et al., 1993) and the early-growth-response 2 (EGR2) gene, a transcription factor that binds to the connexin 32 promoter (Musso et al., 2001).

Genetic linkage analyses have mapped a number of chromosomal loci linked to CMT2 and so far three genes have been identified. Two independent studies have demonstrated an association between mutations in the neurofilament light (NFL) gene and CMT2, thus defining a new disease subtype called CMT2E. In both families, the mutations have autosomal dominant patterns of inheritance (Mersiyanova et al., 2000; De Jonghe et al., 2001). Two additional genes have been linked to CMT2. A mutation with an autosomal dominant pattern of inheritance in the gene encoding the motor protein KIF1Bβ has been linked to CMT2A (Zhao et al., 2001) and a mutation in the gene for lamin A/C, an intermediate filament (IF) protein that is a constituent of the nuclear envelope has been linked to an autosomal recessive form of CMT2 (De Sandre-Giovannoli et al., 2002).

Neurofilaments (NFs) are neuronal-specific IFs with important roles in the development and maintenance of axonal structure (Liem, 1993). NFs are particularly abundant in large myelinated axons and are formed by three subunits, described as high (NFH), medium (NFM), and light (NFL), according to their molecular weights. Like other IF proteins, NF proteins have a tripartite structure, with a central α-helical coil-coiled rod domain that mediates dimerization, and globular N-terminal head and C-terminal tail domains. Rat and mouse NFs are obligate heteropolymers in vivo, requiring the NFL subunit and either the NFM or NFH subunit for the formation of extensive filamentous networks in the absence of other cytoplasmic IFs (Ching and Liem, 1993; Lee et al., 1993). In contrast, human NFL has been reported to self-assemble into a filamentous network (Carter et al., 1998). Mice null for NFL are viable but display a 15-20% reduction in the number of myelinated axons at 2 months of age. They also showed a reduction of axonal diameter and delayed nerve regeneration (Zhu et al., 1997).

In order to investigate the effects of the CMT mutations on

the assembly of NFs, we have conducted transient transfection experiments with wild-type and mutant rat and human NFL cDNAs. The reported mutations are a proline to arginine change in the head domain (P8R) and a glutamine to proline change in the rod domain (Q333P) of the human NFL subunit. A variant (D469N) in the tail domain of NFL has been described while searching for mutations in NFs in amyotrophic lateral sclerosis patients. This variant was not linked to disease (Vechio et al., 1996) and we used it as a control.

Materials and Methods

Construction of plasmids

Rat NFM (rNFM) and NFH (rNFH) cDNAs were cloned in pRSVi vector (Forman et al., 1988) as previously described (Chin and Liem, 1989; Chin and Liem, 1990). The rat NFL (rNFL) cDNA was cloned into the pCI vector (Promega) and constructs for the rNFL variant (D469N), the rNFL P8R mutant and the rNFL Q333P mutant were generated by site-directed mutagenesis, using the QuickChange Mutagenesis Kit (Stratagene) following the manufacturer's instructions. The full-length cDNA of human NFL (hNFL) (GenBank accession no. AY156690) was obtained in a yeast two-hybrid screening using α-internexin as bait and cloned into the pCI vector. We used the Multiple Sequence Alignment (Corpet, 1988) software to align the protein encoded by our hNFL cDNA clone with both the previously published sequence for hNFL and rNFL (Fig. 1A). Sequencing of this clone showed a few differences from the published sequence (GenBank accession no. NM006158). Most of the differences did not change the deduced amino acid sequence and some were reported as single nucleotide polymorphisms (Fig. 1A). Nonetheless, the published clone contained two extra amino acids, Thr153 and Glu166, while our clone possessed an additional serine, located between Ser27 and Val28 of the published hNFL sequence. Four additional amino acid differences were also observed, Gln161Arg, Ala196Arg, Ile453Ser and Ala462Ser. We found a perfect match of our cDNA sequence with the draft sequence of the Human Genome Project (GenBank accession no. AF176680) and the sequence of many human EST clones, including clones with GenBank accession nos. BG425453, BE262311 and BI604227. To further confirm the accuracy of our clone, we obtained another hNFL cDNA by PCR using a human brain QUICK-Clone^{TM} cDNA library (Clontech); the resulting hNFL cDNA is identical to our original hNFL cDNA. For consistency with the published results, we will use the previously reported numbering for hNFL.

The expression constructs for the hNFL variant (D469N), hNFL P8R mutant and hNFL Q333P mutant cDNAs (Fig. 1B) were generated by site-directed mutagenesis using the QuickChange Mutagenesis Kit (Stratagene). The sequences of the resulting clones were confirmed by sequencing. To facilitate simultaneous expression of wild-type and mutant NFL, we generated pCI-hNFL(Q333P)-hNFL(wt) by cloning the PCR fragment that contained the CMV promoter, hNFL(wt) cDNA and SV40 polyA signal into the *Bam*HI site of pCI-hNFL(Q333P). The full-length cDNA of the wild-type hNFM gene was cloned by PCR from a human brain cDNA library (Clontech) using primers hNFM-5′ (5′-gatgagctacacgttggactcgctgggc-aa-3′) and hNFM-3′ (5′-ttagtcactctgggtgacttcctttactat-3′) into the pCR2.1-TOPO vector (Invitrogen), and subsequently cloned into the *Eco*RI site of the pCI vector (Promega). Our clone contained the previously reported Val482Ala polymorphism in the sequence of human NFM (GenBank accession no. NM005382).

Transient transfections

We used two human adrenal carcinoma cells lines described by Sarria et al. (Sarria et al., 1990). SW13 Vim$^+$ cells express endogenous vimentin, while SW13 Vim$^-$ cells are devoid of all cytoplasmic IFs. We maintained the cell lines in DMEM-F12 media supplemented with 10% or 5% fetal bovine serum, respectively, and 1% antibiotic solution (either penicillin-streptomycin or antibiotic-antimycotic) at 37°C and 5% CO_2. Transient transfections were carried out in serum free medium using the GenePORTER system (Gene Therapy Systems) as described in the manufacturer's protocol. For indirect immunofluorescence microscopy, cells were grown on 18-mm glass coverslips. 48 hours after transfection, cells were fixed in methanol at –20°C for 10-15 minutes. and subjected to immunostaining. For western-blot analysis, cells were harvested also at 48 hours post-transfection.

Indirect immunofluorescence microscopy

Immunofluorescence staining started with a blocking step using 10% normal goat serum followed by incubation with the primary antibodies. After washing with PBS, the cells were incubated with appropriate Alexa-Fluor-488 and -594 conjugated secondary antibodies (Molecular Probes) and washed again with PBS. Finally, the coverslips were mounted on slides using Aquamount (Lerner Laboratories) and visualized using a Nikon Eclipse 800 immunofluorescence microscope and a Spot digital camera.

Western blotting

Preparation of cytoskeletal protein extracts using a protease inhibitor cocktail (Roche) was carried out as previously described (Ching and Liem, 1993). The protein fractions were loaded on SDS-PAGE gels and transferred onto PVDF membranes. After a blocking step in PBS-0.05% Tween20 (PBS-T) plus 5% nonfat dry milk, the blots were incubated with primary antibodies in PBS-T plus 5% nonfat dry milk, washed with PBS-T and incubated with 1:10,000 dilution of HRP-conjugated goat anti-rabbit secondary antibody. After further washing with PBS-T, protein detection was carried out using the ECL Detection System (Amersham).

Antibodies

The following primary antibodies were used: mouse anti-NFL monoclonal antibody (clone NR4, Sigma), mouse anti-NFH monoclonal antibody (clone N52, Sigma), mouse anti-NFM monoclonal antibody (clone NN18, Sigma), rabbit anti-NFL and anti-NFM polyclonal antibodies (Kaplan et al., 1991), mouse anti-vimentin monoclonal antibody (clone V9, Sigma), and mouse anti-β-tubulin monoclonal antibody (clone 2-28-33, Sigma).

Statistical analysis

The statistical analysis of the phenotypes observed with transient transfection of the different hNFL cDNAs was carried out using the GraphPad Prism version 3 software. We scored the phenotypes observed in the cells from at least two transient transfection experiments in each case. We compared the percentage of cells displaying each phenotype (Table 1) using an unpaired *t*-test when comparing two groups, and with one-way analysis of variance (ANOVA) followed by the Bonferroni's Multiple Comparison Test when more than two groups were compared. The level of significance was set in all cases at $P<0.05$.

Results

We have conducted transient transfection experiments to determine the effects of CMT2-linked NFL mutations on the formation of IF networks in SW13 Vim$^-$ and SW13 Vim$^+$ cells. Previous studies using the Vim$^-$ cells have shown that rat and mouse neurofilament triplet proteins are obligate heteropolymers in vivo (Ching and Liem, 1993; Lee et al.,

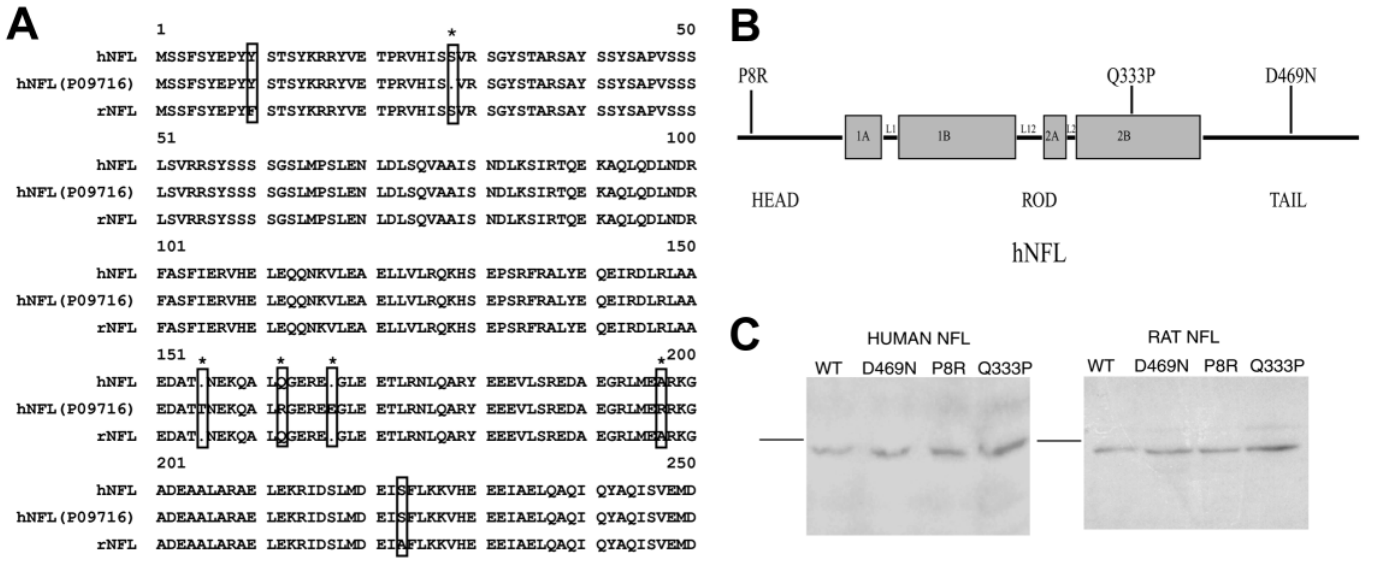

Fig. 1. Sequence alignment of NFL clones, location of mutations and western-blotting of transfected proteins with anti-NFL antibody. (A) Multiple sequence alignment of the hNFL protein encoded by our hNFL cDNA (hNFL), the previously published hNFL sequence (hNFL P09716), and the published rNFL sequence (rNFL). All the differences in the protein sequences are marked by vertical boxes. Differences in the amino acid sequence between hNFL and hNFL (P09716) are marked with an asterisk (*), while amino acids that differ between hNFL and both hNFL (P09716) and rNFL are indicated with a hash mark (#). (B) Schematic representation of NFL protein and the positions of the mutant and variant amino acids. The head, rod and tail domains are indicated. The rod domain is divided into coils 1A, 1B, 2A and 2B separated by linkers L1, L12 and L2. The CMT2 mutations are: P8R in the head domain and Q333P in the coil 2B. The D469N variant is in the tail domain. (C) Western blots of transfected human (left) and rat (right) NFL proteins. Cytoskeletal extracts of transfected cells were separated by SDS-PAGE and subjected to western blotting with a polyclonal anti-NFL antibody. The antibody recognized a band of the same size in wild-type NFL (wt), variant NFL (D469N), head mutant NFL (P8R), and rod mutant NFL (Q333P). The bar indicates the position of the 64 kDa size marker.

1993). In contrast, human NFL was shown to be able to self-assemble into filaments (Carter et al., 1998). This unique self-assembly property of hNFL was thought to be the result of the differences in the primary sequences between human and rodent NFL in the rod domain. We have therefore chosen to investigate the effects of the CMT-linked mutations on the abilities of both rNFL and human hNFL to self-assemble or co-assemble with other IFs. To confirm the expression of full-length NFL proteins in the transfection experiments, the cytoskeletal extracts of transfected wild-type, variant and mutant NFL protein were subjected to Western blotting with a polyclonal anti-NFL antibody. The antibody recognized a band of the same size as the wild-type protein in all the variant and mutant NFL transfectants (Fig. 1C).

Effects of rNFL mutations in NF assembly

The two amino acids that are mutated in CMT2 patients and the one found as a polymorphic variant are conserved between human and rat (Fig. 1A). When either wild-type or the D469N variant rNFL cDNAs were co-transfected in SW13 Vim$^-$ cells with rNFM or rNFH (Fig. 2), the formation of a normal filamentous network was observed. In all subsequent experiments, we never observed a difference between the D469N variant and wild-type NFL. When the P8R mutant rNFL cDNA was co-transfected with rNFM or rNFH, we observed two different phenotypes. Most transfected cells had a filamentous network that tended to bundle (Fig. 3A,B), while in a few cells, the mutant rNFL co-localized with rNFM in cytoplasmic aggregates and no filamentous network was observed (Fig. 3C,D). In contrast, the Q333P mutant rNFL formed aggregates that co-localized with the transfected rNFM (Fig. 3E,F). These aggregates varied in size and distributed throughout the cytoplasm. When the mutant rNFL cDNAs were co-transfected with rNFH, similar results were obtained. The P8R rNFL mutant co-assembled with rNFH into

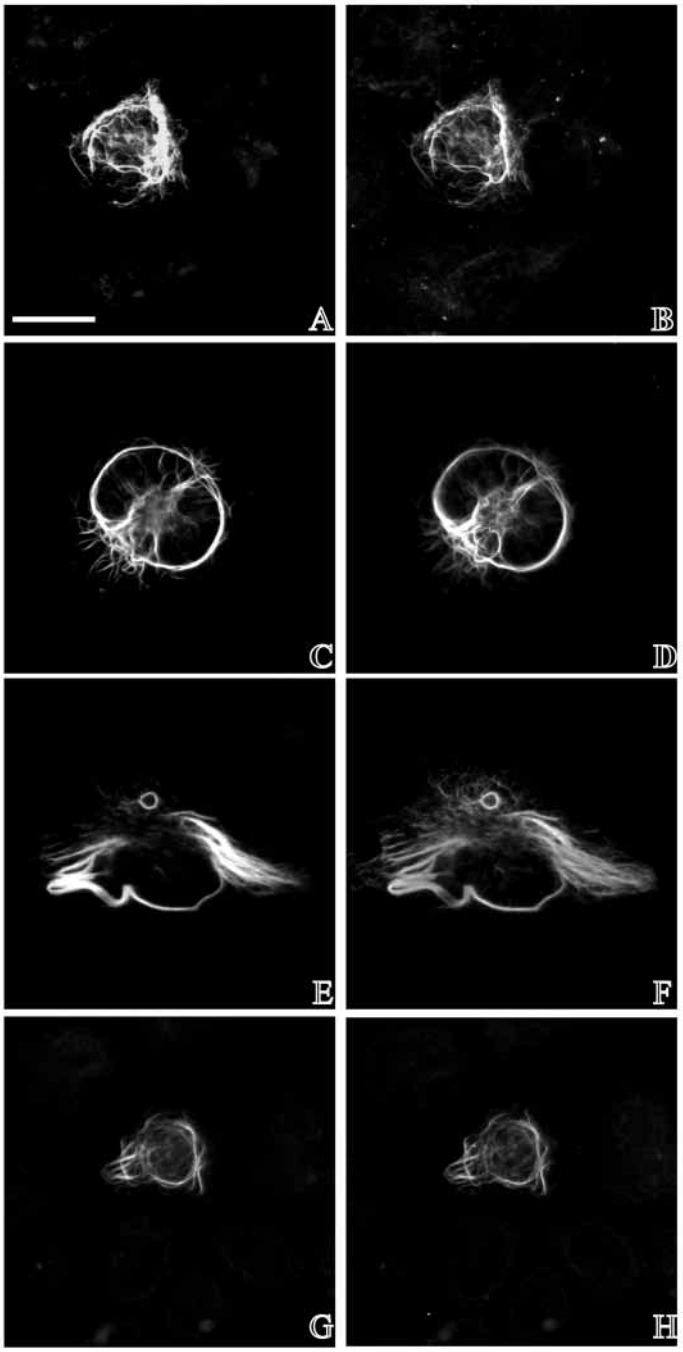

Fig. 2. Co-transfections of wild-type and variant rNFL with rNFM or rNFH in SW13Vim$^-$ cells. (A-D) Rat NFM was co-transfected with wild-type rNFL (A,B) or D469N variant rNFL (C,D). The cells were double-labeled with polyclonal anti-NFL antibody (A,C) and monoclonal anti-NFM antibody (B,D). For both wild-type and variant NFL, a filamentous network throughout the cytoplasm was observed that stained with both antibodies. (E-H) Rat NFH was co-transfected with wild-type rNFL (E,F) or D469N variant rNFL (G,H). The cells were double-labeled with polyclonal anti-NFL antibody (E,G) and monoclonal anti-NFH antibody (F,H). A filamentous network was formed with both wild-type and variant rNFL co-transfected with rNFH. In all the subsequent experiments, the variant NFL behaved identically to wild-type NFL. Bar, 25 μm.

bundles (Fig. 3G,H) or small cytoplasmic aggregates (Fig. 3I,J), whereas the Q333P rNFL mutant formed small aggregates with rNFH resulting in punctate staining (Fig. 3K,L). These results indicate that the CMT2 mutations are able to influence the ability of rNFL to form an intact filamentous network in transfected cells, with the rod mutation having a more dramatic effect (disrupting filament formation) than the head mutation (formation of abnormal thick and bundled filaments).

Effects of CMT2 mutations on hNFL self-assembly

Human NFL has been reported to form homopolymers in vivo, as opposed to rat or mouse NFL (Carter et al., 1998). The authors noted that there were eight differences between rNFL and hNFL in the rod domain. Two of the differences between the rat and human NFL sequences were reported to be important for the ability of hNFL to form a homopolymeric filamentous network in SW13 Vim$^-$ cells; viz. Arg161 (Gln in rat) and the absence of a serine (Ser251 in rat). However, when we cloned the full-length cDNA for hNFL, we found that our cDNA clone had a Gln in position 161, although rat Ser251 was also absent in this hNFL cDNA. The sequence of our NFL cDNA was identical to the NFL draft sequence of the Human Genome Project and also to a number of human EST clones (for more details see Materials and Methods) indicating that the published sequence is likely a variant of hNFL. The phenotypes observed upon single transfection of our hNFL clones are summarized in Table 1. We found that both wild-type and D469N variant hNFL can form homopolymers in SW13 Vim$^-$ cells (Fig. 4A,B and data not shown). We did not observe any statistically significant differences between the phenotypes observed with wild-type hNFL and D469N hNFL (Table 1A). These results suggest that wild-type and D469N hNFL are phenotypically equivalent. An extensive filamentous network was observed only in less than 10% of the transfected cells (Fig. 4B). The most prevalent phenotype was the presence of multiple short and thin filaments (Fig. 4A), which in half of the cells also contained a thicker filamentous core. In all these cases, the cells could not be stained by anti-vimentin antibody, indicating that the observed phenotypes were not due to the occasional revertants of Vim$^-$ cells to Vim$^+$ cells. Therefore, we confirmed that unlike rodent NFL, hNFL is able to self-assemble into filaments, although the hNFL networks were much less extensive than those formed by rNFL/rNFM or rNFL/rNFH (Fig. 2). When we transfected either the P8R (Fig. 4C) or the Q333P (Fig. 4D) hNFL mutants into SW13 Vim$^-$ cells, we found that both mutations abolished the ability of hNFL to self-assemble into a filamentous network. Instead, both mutant hNFL proteins formed aggregates in transfected cells. These observations were statistically significant (Table 1A). Small, dot-like aggregates all around the cytoplasm were observed more frequently with the Q333P hNFL mutant, while one huge aggregate occupying the entire cytoplasm of the cell was observed more frequently with the P8R hNFL mutant.

Since both CMT2 NFL mutations show an autosomal dominant mode of inheritance, we studied the effects of the CMT2-linked hNFL mutations on wild-type hNFL assembly in transfected SW13 Vim$^-$ cells by co-transfecting the wild-

type hNFL with either the D469N variant, the P8R mutant, or the Q333P mutant. Since we were not able to distinguish the wild-type from the mutant hNFL with the available antibodies, we utilized bicistronic hNFL constructs to assure that both wild-type and rod mutant NFL were expressed in the same cells. We have used a similar approach for co-expressing rNFL and rNFH (Leung et al., 1999). The results of the experiment with the bicistronic construct were identical to the results obtained with the co-transfection experiments. Both the P8R mutant hNFL (Fig. 4E) and the Q333P mutant hNFL (Fig. 4F) completely disrupted the formation of wild-type hNFL filaments and caused the formation of aggregates (Table 1B). In contrast, co-transfection of wild-type hNFL with variant D469N hNFL resulted in phenotypes similar to single transfections of either wild-type or D469N hNFL (Table 1B).

Effects of CMT2 linked NFL mutations on co-assembly with hNFM

Although the gene for hNFM is tightly linked with the hNFL gene on chromosome 8p21, no hNFM mutations have so far been described in CMT2 patients. Due to its tight linkage and developmentally coordinated expression with hNFL, we

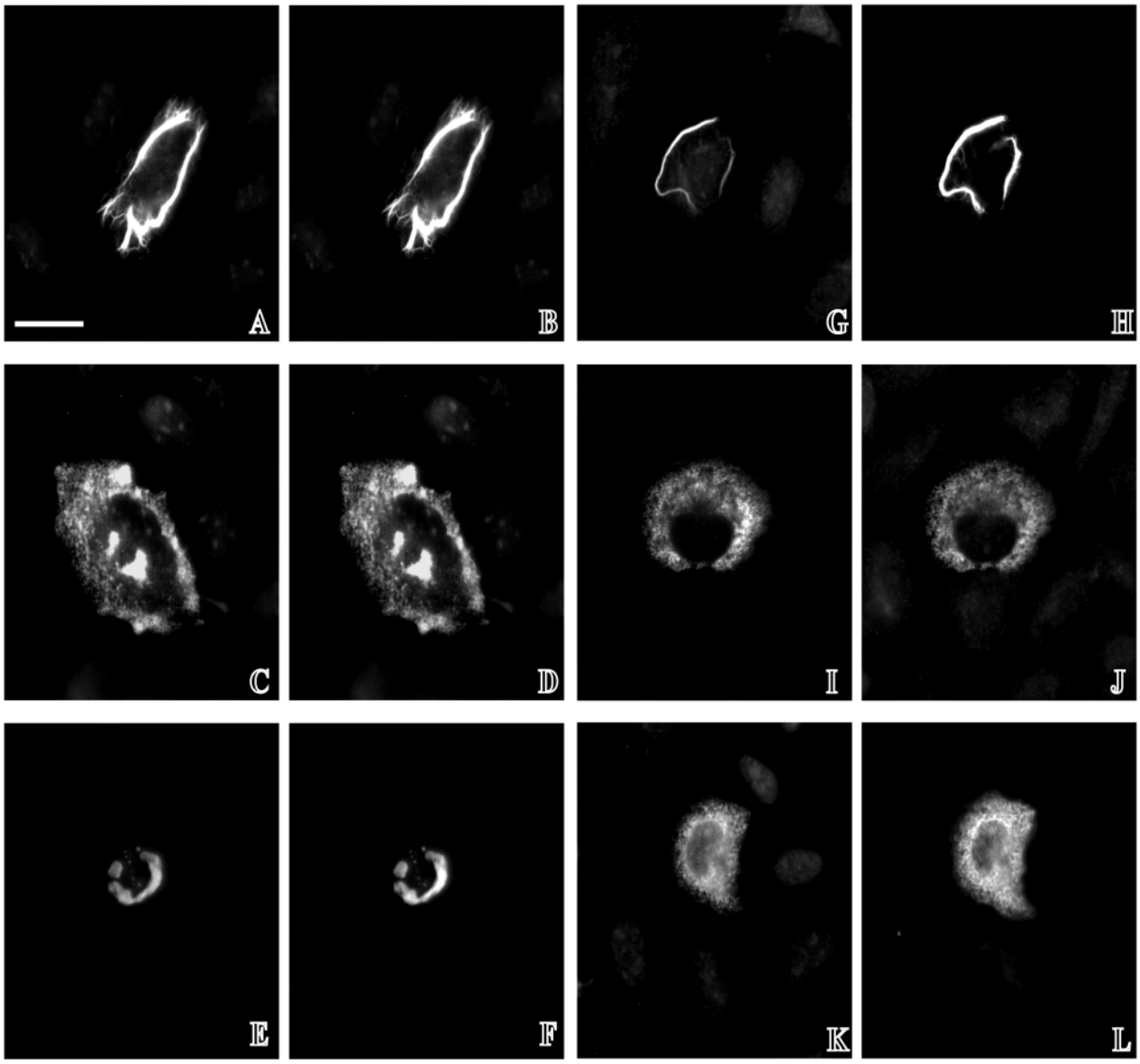

Fig. 3. Co-transfections of mutant rNFL with rNFM or rNFH in SW13 Vim$^-$ cells. (A-F) Rat NFM was co-transfected with P8R mutant rNFL (A-D) and Q333P mutant rNFL (E,F). The cells were double-labeled with polyclonal anti-NFL antibody (A,C,E) and monoclonal anti-NFM antibody (B,D,F). The P8R mutant rNFL co-transfected with rNFM either formed a bundle of filaments (A,B) or displayed punctate or aggregate staining (C,D). The Q333P mutant rNFL resulted in aggregates that contained rNFM (E,F). (G-L) Rat NFH was co-transfected with P8R mutant rNFL (G-J) and Q333P mutant rNFL (K,L). The cells were double-labeled with polyclonal anti-NFL antibody (G,I,K) and monoclonal anti-NFH antibody (H,J,L). The P8R mutant co-assembled into bundled filaments with rNFH in most cases (G,H), or into more punctate material or aggregates (I,J), whereas the Q333P mutant rNFL resulted only in the formation of aggregates with rNFH (K,L). Bar, 25 μm.

selected hNFM to study the effects of hNFL mutations on the formation of filaments in vivo. As observed for rodent NFM, hNFM was not able to self-assemble into filaments (data not shown). The phenotypes observed upon co-transfection of wild-type hNFM with the different hNFL clones are summarized in Table 1C. Wild type hNFL co-transfected with hNFM in SW13 Vim$^-$ cells resulted in the formation of an extensive heteropolymeric filamentous network (Fig. 5A,B). Similar results were obtained with the D469N hNFL variant (data not shown). Transfection of the Q333P mutant hNFL resulted in the formation of aggregates in transfected cells (Fig. 6E,F). These aggregates were distributed throughout the cytoplasm, but could also form larger aggregates. In contrast, when hNFM was co-transfected with the P8R mutant hNFL, we observed that the transfected cells displayed filaments that were bundled, with some individual filaments splaying from the bundle (Fig. 5C,D). Truncated thick filaments could also be observed (cell on the left in Fig. 5C,D). In addition, the P8R mutant hNFL formed aggregates with hNFM in <5% of the transfected cells. Nevertheless, we did not observe the formation of an extensive filamentous network throughout the cytoplasm as in the case of co-transfected wild-type or variant hNFL with hNFM (Fig. 5A,B). These studies

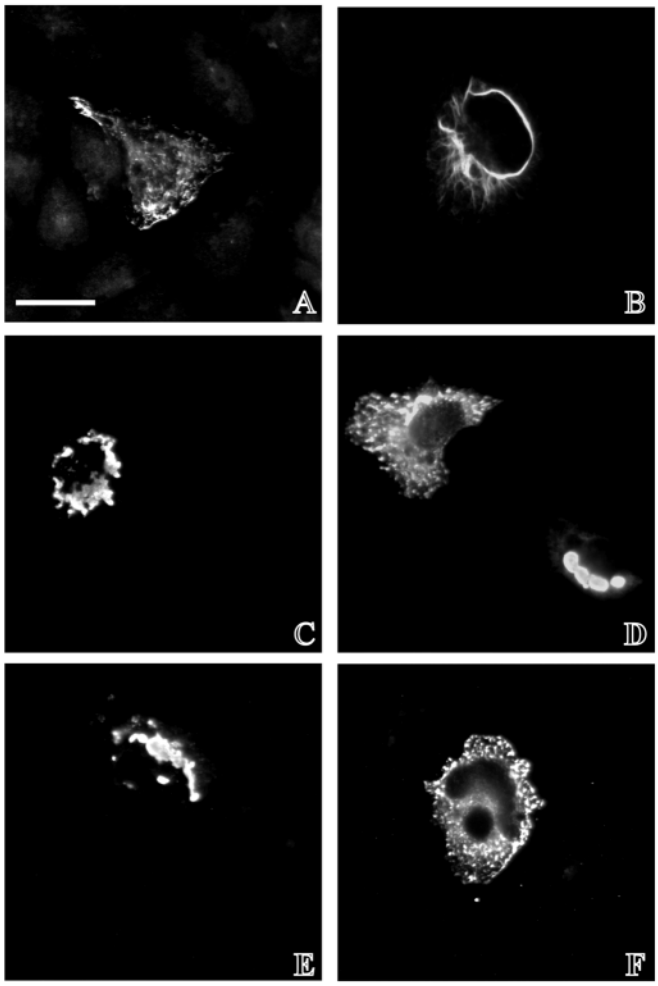

Fig. 4. Transfection of hNFL clones in SW13 Vim$^-$ cells. (A-D) Transient transfection results of wild-type (A,B), P8R mutant (C) and Q333P mutant (D) hNFL. Staining was carried out with monoclonal anti-NFL antibody. Wild-type hNFL generally assembled into short filaments (A), but occasionally also formed a homopolymeric filamentous network (B) that was not stained with anti-vimentin antibody (not shown). The P8R and the Q333P hNFL mutants (C,D) were not capable of self-assembly into a filamentous network, but formed aggregates. (E-F) Co-transfections and staining of wild-type hNFL with the P8R mutant hNFL (E) and Q333P mutant hNFL (F) showed that the mutant proteins disrupted the self-assembly of wild-type hNFL. Results similar to those in F were obtained with a bicistronic construct that expressed both wild-type and Q333P mutant hNFL (not shown). Bar, 25 μm.

Table 1. Classification of the phenotypes observed in transfected cells

A

hNFL	WT	D469N	P8R	Q333P
N	649	354	269	220
Thick filaments	28.35	27.27	0.00*	0.00‡,§
Thin filaments	32.82	24.55	0.00†	0.00¶,**
Mixed filaments	30.05	33.64	0.00†	0.00†
Filamentous network	7.09	2.27	0.00	0.00
Aggregates	1.69	2.27	100.0†	100.0†

B

hNFL(WT)+hNFL	D469N	P8R	Q333P
N	200	123	254
Thick filaments	26.00	0.00	0.00
Thin filaments	38.00	0.00	0.00
Mixed filaments	29.50	0.00	0.00
Filamentous network	5.00	0.00	0.00
Aggregates	1.50	100.0	100.0

C

hNFM(WT)+hNFL	WT	D469N	P8R	Q333P
N	203	180	159	73
Thick filaments	31.53	25.55	72.73	0.00
Thin filaments	38.92	36.67	0.00	0.00
Mixed filaments	29.55	37.78	24.53	0.00
Aggregates	0.00	0.00	3.14	100.0

(A) Percentage of cells transfected with single hNFL constructs displaying each phenotype. *N* represents the total number of cells scored for each transfection. The data were analyzed by using one-way ANOVA followed by the Bonferroni's Multiple comparison test. The level of significance was set at $P<0.05$.

(B) Phenotypes observed in co-transfections of hNFL(WT) with mutant or variant hNFL cDNA. *N* represents the total number of cells scored for each transfection. The data were analyzed by using the unpaired *t*-test. The level of significance was set at $P<0.05$.

(C) Phenotypes observed in co-transfections of hNFL cDNAs with wild-type hNFM. *N* represents the total number of cells scored for each transfection. Co-transfection of hNFM with Q333P hNFL mutant always resulted in the formation of aggregates, while co-transfection with wild-type of D469N variant hNFL always resulted in the formation of a filamentous network, with equal distributions of cells with predominantly thick, thin or mixed filaments. Co-transfection of hNFM with the P8R hNFL mutant resulted in an increased number of cells displaying only thick filaments, while no transfected cells had only thin filaments.

*$P<0.01$ versus WT and D469N.
†$P<0.001$ versus WT and D469N.
‡$P<0.05$ versus D469N.
§$P<0.01$ versus WT.
¶$P<0.01$ versus D469N.
**$P<0.001$ versus WT.

confirm that wild-type and variant hNFL co-transfected with hNFM form a normal filamentous network, whereas the CMT2-linked NFL mutants have varying effects. The Q333P mutant showed a severe ability to disrupt filament formation, resulting in aggregates, whereas the P8R mutant showed a more subtle effect, with NFL/NFM co-polymers appearing as bundled filaments, rather than as a filamentous network.

Effects of hNFL mutations on co-assembly with vimentin

All four hNFL clones were transfected in SW13 Vim^+ cells in order to assess the effects of hNFL mutations on the endogenous vimentin network. Both wild-type hNFL (Fig. 6A,B) and D469N variant hNFL (not shown) co-assembled with the endogenous vimentin network without causing any alterations. The P8R mutant hNFL also co-localized with the endogenous vimentin, although the resulting network was usually not as extensive as observed with the wild-type hNFL (Fig. 6C,D). The effect of the Q333P mutant hNFL on the endogenous vimentin network appeared to be dependent on the relative amounts of vimentin and Q333P hNFL (Fig. 6E-H). When low levels of the Q333P mutant hNFL were expressed, it incorporated into the vimentin network (Fig. 6E,F). As expected due to the inability of the hNFL Q333P mutant to self-assemble, when high levels of Q333P mutant hNFL are expressed, it does not appear to be able to incorporate into the endogenous vimentin network (Fig. 6G,H). Some cells expressing very high levels of mutant protein displayed the co-localization of vimentin with Q333P mutant hNFL in aggregates (not shown).

Effects of transfected hNFL on the microtubule network

NFs have been shown to associate with the microtubule network. In order to investigate the possibility that the microtubules could be disrupted by the overexpression of the mutant hNFL proteins, we transfected wild-type (Fig. 7A), D469N variant (Fig. 7B), P8R mutant (Fig. 7C) and Q333P mutant (Fig. 7D) hNFL constructs into SW13 Vim^- cells and co-stained the cells with anti-β-tubulin and anti-NFL antibodies. Overexpression of hNFL proteins (mutant or wild-type) did not affect the endogenous microtubule network (Fig. 7). Furthermore, transfected SW13 Vim^- cells treated with nocodazole to disrupt the microtubule network also did not show any differences in the NFL networks (mutant or wild-type).

Discusssion

Alterations in the NF network have been identified in transgenic mice overexpressing NFL (Xu et al., 1993). Moreover, experimental mutations (Leu394Pro) in the rod domain of mouse NFL in transgenic mice resulted in severe neurodegeneration of motoneurons, as well as in accumulation of NFs in the perikarya (Lee et al., 1994). The Leu394Pro mutation lies within the LLEGEE sequence (residues 393-398), which signals the end of the rod domain. The first hNFL mutation reported, Q333P (Mersiyanova et al., 2000) is located in coil 2b of the rod domain of NFL that is highly conserved among different species, from Xenopus to humans. Using the MultiCoil Software (Wolf et al., 1997), we found that the Q333P mutation completely eliminated the probability for coiled-coil interactions of amino acid 333 (from 0.981 to 0.000 using the default parameters). This effect is consistent with the observed disruption of the NF network by this mutation. Similar results were observed when we made the same mutation in the rNFL cDNA, confirming that this mutation has a generally serious deleterious effect on filament formation. The Q333P mutation results in the introduction of a 'Pro-kink' in the α-helix, which could have an effect on dimerization (Carter et al., 1998).

The second NFL mutation (P8R) affects the non-α-helical head domain of hNFL (De Jonghe et al., 2001). We used the Network Protein Sequence Analysis software (Combet et al., 2000) to analyze the consensus secondary structure prediction for both mutant hNFL proteins, but we did not find

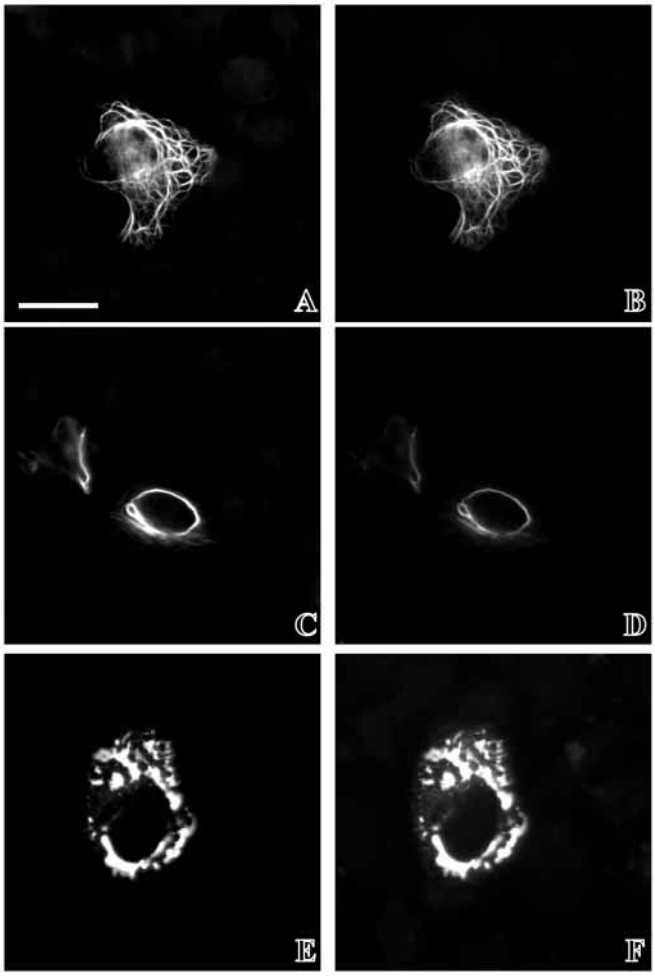

Fig. 5. Co-transfection of hNFL constructs with hNFM in SW13 Vim^- cells. hNFM was co-transfected with either wild-type hNFL (A,B), P8R mutant hNFL (C,D) and Q333P mutant hNFL (E,F). The cells were double-labeled with polyclonal anti-NFL (A,C,E) and monoclonal anti-NFM (B,D,F) antibodies. A filamentous network throughout the cytoplasm was observed for wild-type hNFL and hNFM (A,B). The P8R mutant hNFL formed bundled filaments that stayed on one side of the cell (C,D; cell on the left) or around the nucleus (C,D; cell on the right). The Q333P mutant NFL always formed aggregates with hNFM (E,F). Bar, 25 μm.

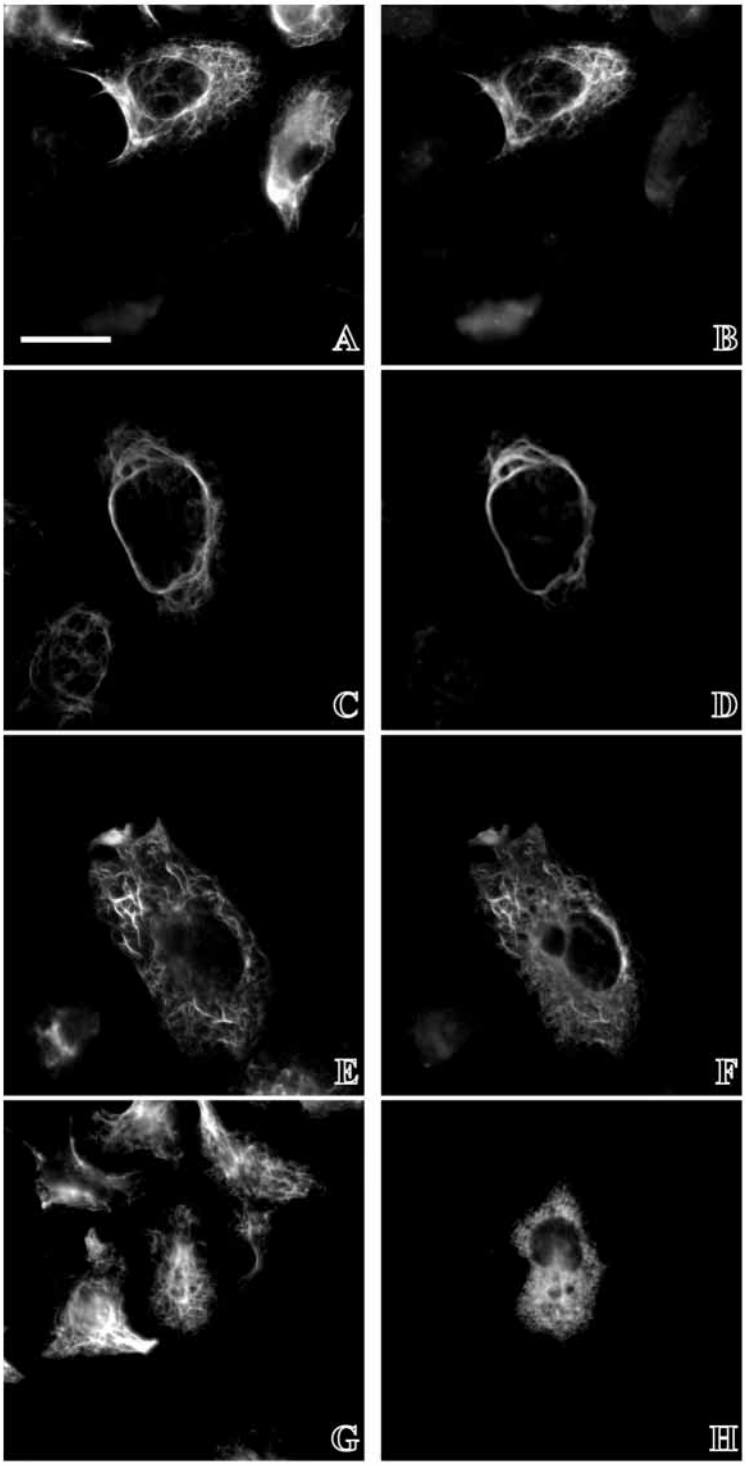

Fig. 6. Transient transfection of hNFL constructs in SW13 Vim$^+$ cells. Transfection of wild-type (A,B), P8R mutant (C,D) and Q333P mutant (E-H) hNFL. The cells were double-labeled with monoclonal anti-vimentin (A,C,E,G) and polyclonal anti-NFL (B,D,F,H) antibodies. Both wild-type hNFL (A,B) and D469 hNFL (not shown) incorporated into the endogenous vimentin network. The P8R mutant hNFL protein incorporated into the endogenous vimentin network in most cases (C,D). The co-assembly of the Q333P mutant hNFL with endogenous vimentin was dependent on their relative levels of expression (E-H). At lower levels of expression the mutant Q333P hNFL incorporated into the vimentin network (E,F), while at higher levels of expression it aggregated in the cytoplasm (G,H). Bar, 25 μm.

any differences due to both the P8R and the Q333P mutations. Using the NetPhos 2.0 Prediction server (Blom et al., 1999) we determined that the P8R mutation results in the appearance of a new potential phosphorylation site (Ser11), for both protein kinase A and casein kinase-II. Since phosphorylation of the head domain of NFL regulates its assembly and disassembly (Nakamura et al., 2000; Sihag and Nixon, 1989; Sihag and Nixon, 1991), the possibility exists that changes in the phosphorylation of the head domain of hNFL might be involved in the effects caused by the hNFL P8R mutation in the assembly of IFs. Deletion analysis has demonstrated that the head domain of NFL is required for filament assembly (Ching and Liem, 1998). However, the contribution of individual amino acids of the head domain to filament formation has not been fully determined. The P8R mutation had a less severe effect on filament formation than the Q333P mutant NFL. Unlike wild-type or variant hNFL, the P8R mutant hNFL was not able to self-assemble. However, it co-assembled with hNFM into filaments, although these filaments had a tendency to form bundles. Similar results were also obtained with the corresponding mutation in rNFL. Moreover, the P8R mutant rNFL colocalized with rNFM or rNFH in cytoplasmic aggregates in a small percentage of transfected cells. Some studies have suggested that bundled NFs may undergo transport at a slower rate than individual filaments (Yabe et al., 2001). Although these studies were carried out using NFs that were highly phosphorylated in the carboxyl-terminal domain, it is possible that this could also apply to the case of the NF bundles caused by the P8R hNFL mutation.

Our transfection data suggest that both CMT2-linked mutations in NFL influence the abilities of these proteins to assemble into filaments. Neither human NFL mutant was able to self-assemble in SW13 Vim$^-$ cells. In contrast, wild-type or variant hNFL generally self-assembled into short filaments and more rarely into an extensive filamentous network. In co-assembly studies aggregates were formed when either the rat or human Q333P mutant NFL was co-expressed with the other NF proteins. The P8R mutant NFL tended to form bundles of filaments or aggregates, rather than an extensive filamentous network when co-transfected with NFM or NFH. We do not yet know how these effects ultimately lead to neurodegeneration in CMT2E patients, but it is possible that the resulting aggregated or bundled neurofilaments affect the axoplasmic transport of the proteins. Recently, it was shown that KIF1Bβ$^{+/-}$ mice have a defect in transporting synaptic vesicle precursors and suffer from progressive muscle weakness similar to human CMT2. A mutation in the motor domain of KIF1Bβ was identified in families affected with CMT2A and previously assigned by linkage analysis to the interval containing the KIF1Bβ gene (Zhao et al., 2001). We believe the results described here will have an impact on the investigations regarding the pathogenic mechanisms involved in CMT, and possibly in other neurodegenerative diseases as well.

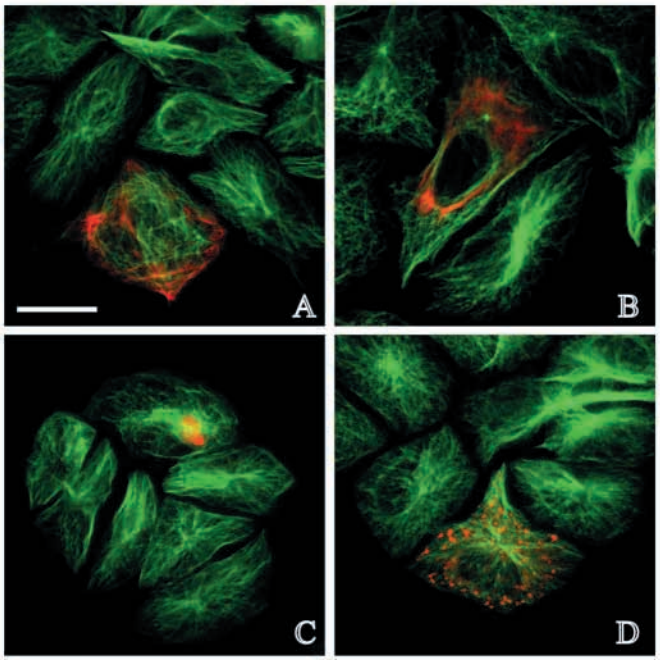

Fig. 7. Transfection of hNFL does not affect the microtubule network of SW13 Vim⁻ cells. Transient transfection of wild-type hNFL (A), D469N variant hNFL (B), P8R mutant hNFL (C) and Q333P mutant hNFL (D) into SW13 Vim⁻ cells. Cells were co-stained with monoclonal anti-β-tubulin antibody (green) and polyclonal anti-NFL antibody (red). Shown are the merged images corresponding to staining with both antibodies. Transfection of hNFL constructs did not affect the microtubule network, and NFL and tubulin did not co-localize.

We thank members of the Liem laboratory and especially G. Y. Ching for helpful discussions. The help of M. A. Lopez-Toledano (Columbia University) with the statistical analysis of the data is appreciated. This work was supported by grant NS15182. R.P.O. is a post-doctoral fellow of the Charcot-Marie-Tooth Association and C.L.L. was a post-doctoral trainee on training grant AG00189. We are indebted to Robert Evans (University of Colorado) for the gift of the SW13 cells.

References

Bergoffen, J., Scherer, S. S., Wang, S., Scott, M. O., Bone, L. J., Paul, D. L., Chen, K., Lensch, M. W., Chance, P. F. and Fischbeck, K. H. (1993). Connexin mutations in X-linked Charcot-Marie-Tooth disease. *Science* **262**, 2039-2042.

Blom, N., Gammeltoft, S. and Brunak, S. (1999). Sequence and structure-based prediction of eukaryotic protein phosphorylation sites. *J. Mol. Biol.* **294**, 1351-1362.

Carter, J., Gragerov, A., Konvicka, K., Elder, G., Weinstein, H. and Lazzarini, R. A. (1998). Neurofilament (NF) assembly; divergent characteristics of human and rodent NF-L subunits. *J. Biol. Chem.* **273**, 5101-5108.

Chin, S. S. and Liem, R. K. (1989). Expression of rat neurofilament proteins NF-L and NF-M in transfected non-neuronal cells. *Eur. J. Cell Biol.* **50**, 475-490.

Chin, S. S. and Liem, R. K. (1990). Transfected rat high-molecular-weight neurofilament (NF-H) coassembles with vimentin in a predominantly nonphosphorylated form. *J. Neurosci.* **10**, 3714-3726.

Ching, G. Y. and Liem, R. K. (1993). Assembly of type IV neuronal intermediate filaments in nonneuronal cells in the absence of preexisting cytoplasmic intermediate filaments. *J. Cell Biol.* **122**, 1323-1335.

Ching, G. Y. and Liem, R. K. (1998). Roles of head and tail domains in alpha-internexin's self-assembly and coassembly with the neurofilament triplet proteins. *J. Cell Sci.* **111**, 321-333.

Combet, C., Blanchet, C., Geourjon, C. and Deleage, G. (2000). NPS@: network protein sequence analysis. *Trends Biochem. Sci.* **25**, 147-150.

Corpet, F. (1988). Multiple sequence alignment with hierarchical clustering. *Nucleic Acids Res* **16**, 10881-10890.

De Jonghe, P., Mersivanova, I., Nelis, E., del Favero, J., Martin, J. J., van Broeckhoven, C., Evgrafov, O. and Timmerman, V. (2001). Further evidence that neurofilament light chain gene mutations can cause Charcot-Marie-Tooth disease type 2E. *Ann. Neurol.* **49**, 245-249.

De Sandre-Giovannoli, A., Chaouch, M., Kozlov, S., Vallat, J. M., Tazir, M., Kassouri, N., Szepetowski, P., Hammadouche, T., Vandenberghe, A., Stewart, C. L. et al. (2002). Homozygous defects in LMNA, encoding lamin A/C nuclear-envelope proteins, cause autosomal recessive axonal neuropathy in human (Charcot-Marie-Tooth disorder type 2) and mouse. *Am. J. Hum. Genet.* **70**, 726-736.

Forman, B. M., Yang, C. R., Stanley, F., Casanova, J. and Samuels, H. H. (1988). c-erbA protooncogenes mediate thyroid hormone-dependent and independent regulation of the rat growth hormone and prolactin genes. *Mol. Endocrinol.* **2**, 902-911.

Hayasaka, K., Himoro, M., Sato, W., Takada, G., Uyemura, K., Shimuzu, N., Bird, T. D., Connealy, P. M. and Chance, P. F. (1993). Charcot-Marie-Tooth neuropathy type 1B is associated with mutations of the myelin P0 gene. *Nat. Genet.* **5**, 31-34.

Kaplan, M. P., Chin, S. S., Macioce, P., Srinawasan, J., Hashim, G. and Liem, R. K. (1991). Characterization of a panel of neurofilament antibodies recognizing N- terminal epitopes. *J. Neurosci. Res.* **30**, 545-554.

Lee, M. K., Xu, Z., Wong, P. C. and Cleveland, D. W. (1993). Neurofilaments are obligate heteropolymers in vivo. *J. Cell Biol.* **122**, 1337-1350.

Lee, M. K., Marszalek, J. R. and Cleveland, D. W. (1994). A mutant neurofilament subunit causes massive, selective motor neuron death: implications for the pathogenesis of human motor neuron disease. *Neuron* **13**, 975-988.

Leung, C. L., Sun, D. and Liem, R. K. H. (1999). The intermediate filament protein peripherin is the specific interaction partner of mouse BPAG1-n (dystonin) in neurons. *J. Cell Biol.* **144**, 435-446.

Liem, R. K. (1993). Molecular biology of neuronal intermediate filaments. *Curr. Opin. Cell Biol.* **5**, 12-16.

Mersiyanova, I. V., Perepelov, A. V., Polyakov, A. V., Sitnikov, V. F., Dadali, E. L., Oparin, R. B., Petrin, A. N. and Evgrafov, O. V. (2000). A new variant of Charcot-Marie-Tooth disease type 2 is probably the result of a mutation in the neurofilament-light gene. *Am. J. Hum. Genet.* **67**, 37-46.

Musso, M., Balestra, P., Bellone, E., Cassandrini, D., di Maria, E., Doria, L. L., Grandis, M., Mancardi, G. L., Schenone, A., Levi, G. et al. (2001). The D355V mutation decreases EGR2 binding to an element within the Cx32 promoter. *Neurobiol. Dis.* **8**, 700-706.

Nakamura, Y., Hashimoto, R., Kashiwagi, Y., Aimoto, S., Fukusho, E., Matsumoto, N., Kudo, T. and Takeda, M. (2000). Major phosphorylation site (Ser55) of neurofilament L by cyclic AMP- dependent protein kinase in rat primary neuronal culture. *J. Neurochem.* **74**, 949-959.

Roa, B. B., Garcia, C. A., Pentao, L., Killian, J. M., Trask, B. J., Suter, U., Snipes, G. J., Ortiz-Lopez, R., Shooter, E. M., Patel, P. I. et al. (1993). Evidence for a recessive PMP22 point mutation in Charcot-Marie-Tooth disease type 1A. *Nat. Genet.* **5**, 189-194.

Sarria, A. J., Nordeen, S. K. and Evans, R. M. (1990). Regulated expression of vimentin cDNA in cells in the presence and absence of a preexisting vimentin filament network. *J. Cell Biol.* **111**, 553-565.

Sihag, R. K. and Nixon, R. A. (1989). In vivo phosphorylation of distinct domains of the 70-kilodalton neurofilament subunit involves different protein kinases. *J. Biol. Chem.* **264**, 457-464.

Sihag, R. K. and Nixon, R. A. (1991). Identification of Ser-55 as a major protein kinase A phosphorylation site on the 70-kDa subunit of neurofilaments. Early turnover during axonal transport. *J. Biol. Chem.* **266**, 18861-18867.

Vechio, J. D., Bruijn, L. I., Xu, Z., Brown, R. H., Jr and Cleveland, D. W. (1996). Sequence variants in human neurofilament proteins: absence of linkage to familial amyotrophic lateral sclerosis. *Ann. Neurol.* **40**, 603-610.

Warner, L. E., Garcia, C. A. and Lupski, J. R. (1999). Hereditary peripheral neuropathies: clinical forms, genetics, and molecular mechanisms. *Annu. Rev. Med.* **50**, 263-275.

Wolf, E., Kim, P. S. and Berger, B. (1997). MultiCoil: a program for predicting two- and three-stranded coiled coils. *Protein Sci.* **6**, 1179-1189.

Xu, Z., Cork, L. C., Griffin, J. W. and Cleveland, D. W. (1993). Increased expression of neurofilament subunit NF-L produces morphological

alterations that resemble the pathology of human motor neuron disease. *Cell* **73**, 23-33.

Yabe, J. T., Chylinski, T., Wang, F. S., Pimenta, A., Kattar, S. D., Linsley, M. D., Chan, W. K. and Shea, T. B. (2001). Neurofilaments consist of distinct populations that can be distinguished by C-terminal phosphorylation, bundling, and axonal transport rate in growing axonal neurites. *J. Neurosci.* **21**, 2195-2205.

Zhao, C., Takita, J., Tanaka, Y., Setou, M., Nakagawa, T., Takeda, S., Yang, H. W., Terada, S., Nakata, T., Takei, Y. et al. (2001). Charcot-Marie-Tooth disease type 2A caused by mutation in a microtubule motor KIF1Bbeta. *Cell* **105**, 587-597.

Zhu, Q., Couillard-Despres, S. and Julien, J. P. (1997). Delayed maturation of regenerating myelinated axons in mice lacking neurofilaments. *Exp. Neurol*. **148**, 299-316.